

Sensor and Simulation Notes

Note 448

3 July 2000

Symmetry in Single-Polarization Reflector Impulse-Radiating Antennas

Carl E. Baum  
Air Force Research Laboratory  
Directorate Energy Directorate

Abstract

There are various construction details for reflector impulse-radiating antennas (IRAs) which limit the achievement of the ideal performance characteristics. Symmetry planes are important for polarization purity in the direction of the main beam. This involves details of the feed cables, possible inclusion of a ground plane perpendicular to the ideal electric field, and location of perturbations in low-field regions. Another symmetry concerns the balancing of the low-frequency electric and magnetic dipoles by including special structures connected to the feed arms.

---

This work was sponsored in part by the Air Force Office of Scientific Research, and in part by the Air Force Research Laboratory, Directed Energy Directorate.

## 1. Introduction

Impulse-radiating antennas (IRA) have many applications and a large literature has developed [18]. For some applications (e.g., polarimetry) a controlled frequency-independent polarization is important [10, 11]. An important technique for polarization control is symmetry in the antenna geometry. Here our attention is directed to polarization on the beam center which can be a symmetry axis for the antenna.

The present paper can be considered an extension of [5] where various features (including symmetry) of the TEM feed of a reflector IRA are considered. Besides the general overall geometry of the IRA, now smaller pieces are considered for their effects on the symmetry. These include especially the signal cables including their locations relative to the other conductors. Inevitably some small asymmetries will be present, but the effects of these can be minimized by judicious positioning of the signal cables, and by the positioning of conductors which minimize undesirable field components. Note that here we are not considering high-voltage operation with, say, a spark gap at the focal point. Rather we are considering a low-voltage type with two  $100 \Omega$  feed cables from a single  $50 \Omega$  cable as discussed in [5 (Fig. 4.1B)].

Another symmetry considered is that of duality (in the Maxwell equations) as applied to the low-frequency electric- and magnetic-dipole moments so as to better achieve the desirable balance between these two.

## 2. Symmetry Planes

Fundamental to the design of such reflector IRAs is symmetry planes and the division of electromagnetic fields into symmetric and antisymmetric parts which do not interact with each other [14, 17]. Figure 2.1 shows a four-arm reflector IRA (front view) with beam center on the +z axis. By placing the four identical arms on planes defined by

$$\phi = \phi_0, \pi - \phi_0, \pi + \phi_0, 2\pi - \phi_0 \quad (2.1)$$

(for arms labeled 1 through 4 respectively) in the cylindrical  $(\Psi, \phi, z)$  coordinate system defined by

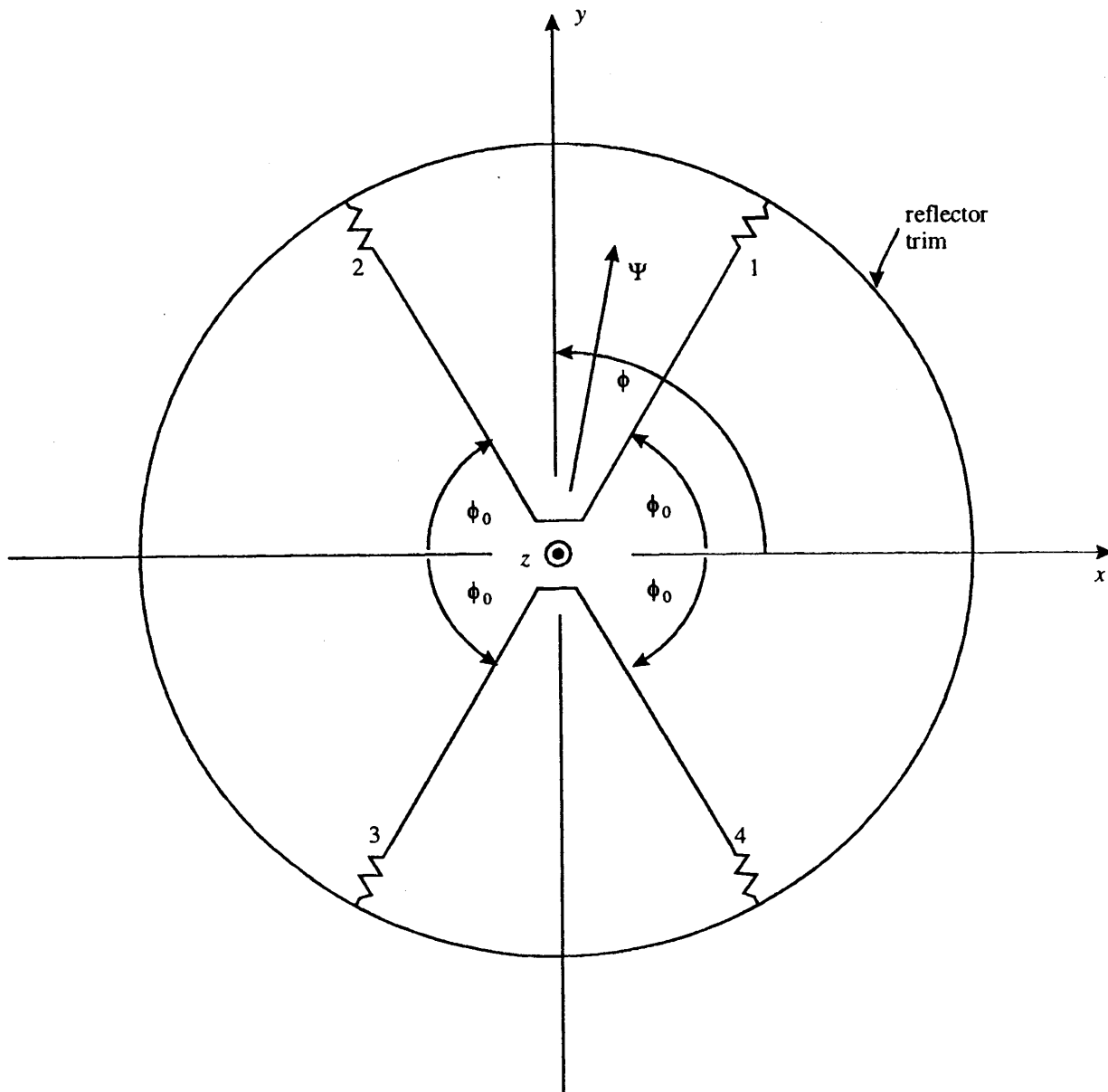
$$x = \Psi \cos(\phi), \quad y = \Psi \sin(\phi) \quad (2.2)$$

the antenna can be constructed with two symmetry planes: the  $y = 0$  plane with respect to which the fields (in transmission) are symmetric, and the  $x = 0$  plane with respect to which the same fields are antisymmetric. The four terminating resistors are typically each  $200 \Omega$  to match a  $200 \Omega$  conical transmission line. This in turn matches the series combination of two  $100 \Omega$  coaxes per the technique in [5 (fig. 4.1B)]. These cables are not shown in the figure.

With only one of the two aforementioned planes as a symmetry plane the fields in transmission on the z axis have pure vertical polarization. Of course, real antennas are not constructed perfectly, so two symmetry planes as in Fig. 2.1 can improve the polarization purity on the z axis. Note that the symmetry planes are associated with the groups (dyadic representation) as

$$\begin{aligned} R_x &= \left\{ \begin{array}{c} \leftrightarrow \\ 1 \end{array}, \begin{array}{c} \leftrightarrow \\ R_x \end{array} \right\}, \quad \begin{array}{c} \leftrightarrow^2 \\ R_x = 1 \end{array} \\ \begin{array}{c} \leftrightarrow \\ 1 \end{array} &= \begin{array}{c} \rightarrow \\ 1_x \end{array} \begin{array}{c} \rightarrow \\ 1_x \end{array} + \begin{array}{c} \rightarrow \\ 1_y \end{array} \begin{array}{c} \rightarrow \\ 1_y \end{array} + \begin{array}{c} \rightarrow \\ 1_z \end{array} \begin{array}{c} \rightarrow \\ 1_z \end{array} = \begin{pmatrix} 1 & 0 & 0 \\ 0 & 1 & 0 \\ 0 & 0 & 1 \end{pmatrix} \equiv \text{identity} \\ R_x &= \begin{array}{c} \leftrightarrow \\ 1 \end{array} - 2 \begin{array}{c} \rightarrow \\ 1_x \end{array} \begin{array}{c} \rightarrow \\ 1_x \end{array} = \begin{pmatrix} -1 & 0 & 0 \\ 0 & 1 & 0 \\ 0 & 0 & 1 \end{pmatrix} \equiv \text{reflection through } x = 0 \text{ plane} \\ R_y &= \left\{ \begin{array}{c} \leftrightarrow \\ 1 \end{array}, \begin{array}{c} \leftrightarrow \\ R_y \end{array} \right\}, \quad \begin{array}{c} \leftrightarrow^2 \\ R_y = 1 \end{array} \\ R_y &= \begin{array}{c} \leftrightarrow \\ 1 \end{array} - 2 \begin{array}{c} \rightarrow \\ 1_y \end{array} \begin{array}{c} \rightarrow \\ 1_y \end{array} = \begin{pmatrix} 1 & 0 & 0 \\ 0 & -1 & 0 \\ 0 & 0 & 1 \end{pmatrix} \equiv \text{reflection through } y = 0 \text{ plane} \end{aligned} \quad (2.3)$$

Adjoining these two groups gives the four-element group



Feed cables are not shown

Fig. 2.1 Four-Arm Reflector IRA With Two Symmetry Planes

$$C_{2a} = R_x \otimes R_y = \left\{ \begin{array}{c} \leftrightarrow \\ \leftrightarrow \\ \leftrightarrow \\ \leftrightarrow \end{array} \cdot \begin{array}{c} \leftrightarrow \\ \leftrightarrow \\ \leftrightarrow \\ \leftrightarrow \end{array} \right\} \\ \begin{array}{c} \leftrightarrow \\ \leftrightarrow \\ \leftrightarrow \\ \leftrightarrow \end{array} \cdot \begin{array}{c} \leftrightarrow \\ \leftrightarrow \\ \leftrightarrow \\ \leftrightarrow \end{array} = \begin{array}{c} \leftrightarrow \\ \leftrightarrow \\ \leftrightarrow \\ \leftrightarrow \end{array} \cdot \begin{array}{c} \leftrightarrow \\ \leftrightarrow \\ \leftrightarrow \\ \leftrightarrow \end{array} \equiv I_z = \begin{pmatrix} -1 & 0 & 0 \\ 0 & -1 & 0 \\ 0 & 0 & 1 \end{pmatrix} \quad (2.4)$$

$\equiv$  inversion transverse to  $z$  axis or  $\pi(180^\circ)$  rotation about  $z$  axis

This defines the  $z$  axis as a 2-fold rotation axis as indicated by  $C_2$  with (in addition) two axial symmetry planes or  $C_{2a}$ .

While the fields incident on the antenna (in reception) have, in general, both symmetric and antisymmetric parts with respect to the various symmetry planes, reciprocity assures us that the polarization in transmission is also the polarization in reception. Furthermore, a symmetry plane in the antenna implies the same symmetry in the pattern, applying to both transmission and reception. So, polarization purity is also present on the symmetry planes in the pattern.

Note that  $\phi_o$  is not specified here. Early designs had  $\phi_o = \pi/4$  ( $45^\circ$ ) due to the simple parallel addition of two  $400 \Omega$  edge-on feed-arm pairs which do not interact with each other (one feed-arm pair being perpendicular to the electric field from the other feed-arm pair). More recently [9, 12] calculations which allow  $\phi_o$  to take on other values have been performed showing some improved performance for somewhat larger  $\phi_o$ , while keeping the  $200 \Omega$  feed impedance. For the present discussion the symmetrical positioning of the arms with respect to the two symmetry planes is of great importance.

While, as in Fig. 2.1, the paraboloidal reflector has a circular rim, the truncation of the reflector can have other shapes of rims as projected on the  $z = 0$  plane for various applications [13]. In keeping with the symmetries discussed here, one can easily have the  $x = 0$  and/or  $y = 0$  planes as symmetry planes. One example is a rectangular aperture [13].

Now let us consider the positioning of the signal cables. Figure 2.2 shows a blowup of the region where the feed arms approach the paraboloid focal point. Here we have one  $100 \Omega$  coax on the  $z$  axis with center conductor connecting to arms 3 and 4. The other coax is bonded to arm 2 with center conductor passing through a hole in the connection between arms 1 and 2 to reach the shield of the other coax. As the coax on arm 2 approaches the focus the outer-conductor diameter may eventually approach or even exceed the width of the flat-plate cone (apex at the focus). This is eventually truncated before reaching the focus and electrically connected to arm 1 by a

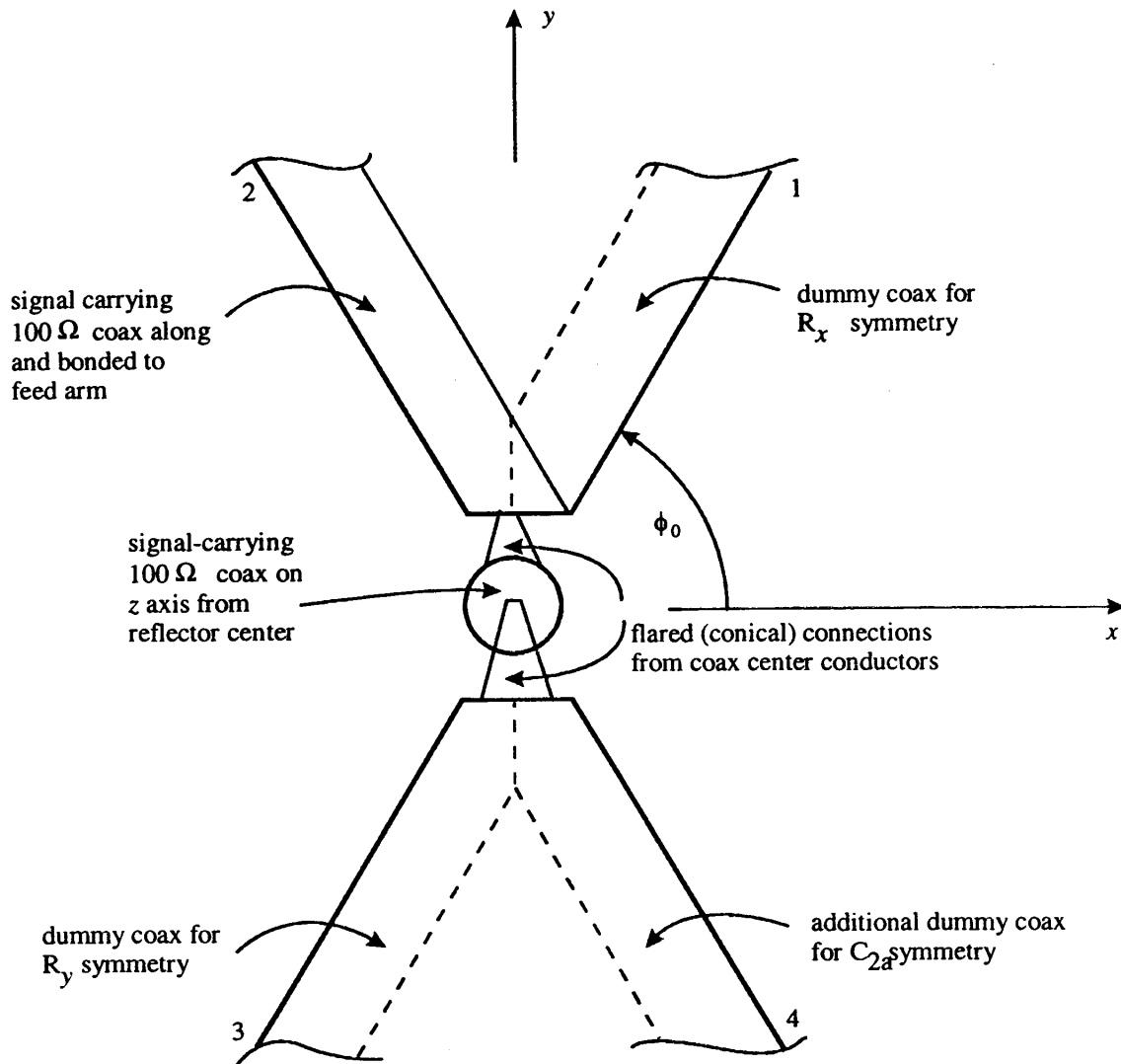


Fig. 2.2 Addition of Dummy Coaxes to Give More Accurate Symmetry Planes

flat piece of metal parallel to the  $y = 0$  plane. The presence of this coax (and its connection through to the shield of the other coax) is a necessary perturbation of the ideal geometry. One can make this coax as small in diameter (in the region near the focus) as practical. In order to remove the asymmetry associated with this coax outer shield, one can add other dummy coaxes (or just conducting tubes of the same outer diameter) at appropriate symmetrical locations.

In order to preserve the  $R_x$  symmetry, one can add such a dummy on arm 1. For  $R_y$  symmetry one can be added on arm 3. For preserving both symmetry planes ( $C_{2a}$  symmetry) one can add, in addition, a third dummy on arm 4.

Another aspect of antenna symmetry concerns the connection of signal cables and other conductors (and to a lesser degree dielectrics) to the antenna. In particular, the typically 50  $\Omega$  coax, which divides (parallel connection) behind the reflector into two 100  $\Omega$  coaxes, will be general scatter the fields. So this cable should be positioned on any symmetry planes of the antennas. For two symmetry planes this implies that this cable should lie on the antenna axis ( $z$  axis). Since the junction to the 100  $\Omega$  coaxes (for minimum length) is not on the antenna axis, the 50  $\Omega$  cable should be routed along the reflector back surface until the antenna axis is reached as indicated in Fig. 2.3. At this point, the 50  $\Omega$  cable is bent to leave the antenna via the (negative)  $z$  axis. Note that all three cables should be bonded (or very frequently electrically connected) to the back of the reflector so that these cable shields are topologically part of the reflector surface, and only small perturbations on it [16]. Especially on the  $z$  axis there should be a good electrical connection from the 50  $\Omega$  cable shield to the reflector.

For various instrumentation reasons the 50  $\Omega$  cable and/or conductors connected to it will, in general, need to depart from the  $z$  axis. Also, other scatterers will generally be in proximity to the antenna and will scatter fields which interact with the cable shield. So, some improvement may be expected by the addition of chokes to suppress such external shield currents as indicated in Fig. 2.3.

Recall the choke on one of the 100  $\Omega$  cables as it passes by one of the four terminating resistors. No choke is perfect, but has some finite inductance. If this is a problem, especially at low frequencies, inducing a lack of symmetry in the antenna feed, then symmetry can be restored by introducing one or more similar impedances in parallel with the other terminating resistors.

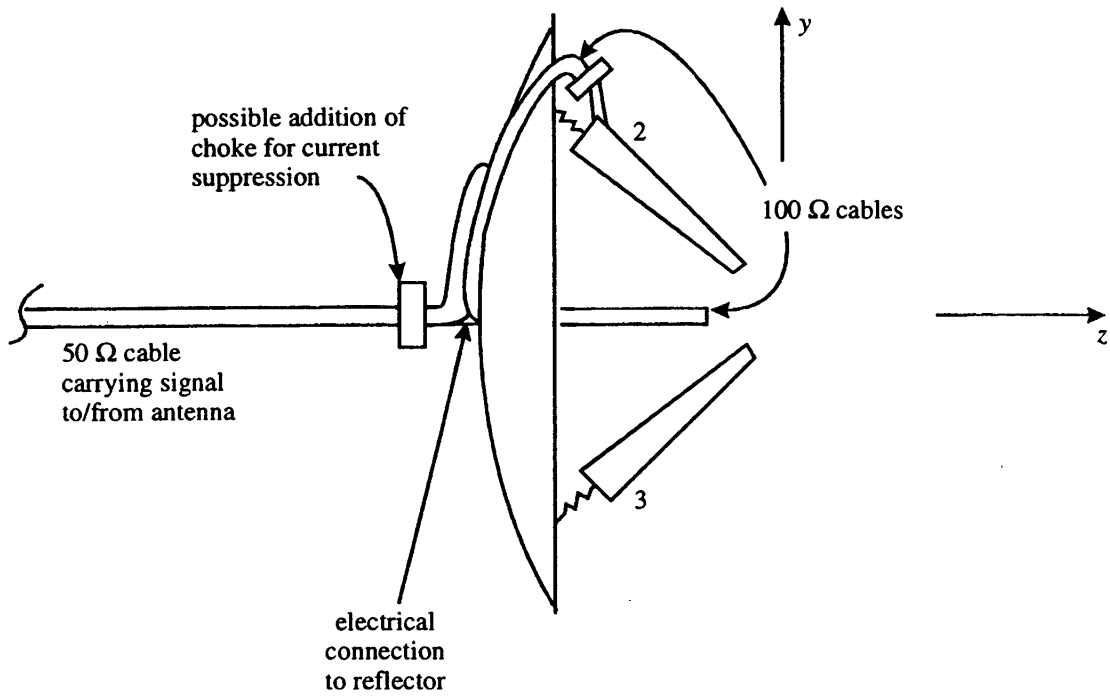


Fig. 2.3 Symmetric Positioning of 50 Ω Cable Connection to Antenna



### 3. Additional Suppression of Crosspol on Axis

With symmetry as a basic design principle, the crosspol on axis (beam center) is ideally zero. However, various details of construction invariably introduce asymmetries. One then needs to consider various ways to make such asymmetries less significant.

Suppose, for example, that the currents on the feed arms are not all exactly the same. Returning to Fig. 2.1, suppose that the currents on arms 1 and 2 are slightly different. As one increases  $\phi_0$  toward  $\pi/2$  ( $90^\circ$ ) the two arms are merged into one and the symmetry ( $x = 0$  plane) is restored. So increasing  $\phi_0$  from the traditional angle of  $\pi/4$ , in general, increases the polarization purity on axis.

Another technique for minimizing the effects of asymmetries is to place such objects in low-field regions of the antenna so that the scattering by such symmetry-perturbing objects is minimized. As an example, returning to Fig. 2.2, consider the signal cable bonded to feed arm 2. Arms 1 and 2 being fed in parallel the fields between them are small compared to the fields between this arm pair and the arm pair comprising arms 3 and 4. So one should place the 100  $\Omega$  signal carrying coax on arm 2 on the side facing arm 1. Note also that as  $\phi_0$  is increased the field near the coax is further reduced.

Going further, this 100  $\Omega$  feed coax is only a small perturbation on feed arm 2 near termination resistor 2. As the cable progresses toward the focal point it becomes a larger and larger perturbation to the arm geometry, and may eventually be of comparable size. This effect can be minimized by transitioning between different diameters of 100  $\Omega$  coax, using a very small diameter for a short length near the focus, but a larger diameter with lower loss for most of the distance back to the 50  $\Omega$  coax.

Yet another technique for minimizing the effects of asymmetries involves suppression of the resulting asymmetric field components in antenna transmission. Where some electric-field component is supposed to be zero one can place thin conductors to force such field components to (near) zero. A well-known example of this [5] consists of a metal sheet about which the fields are antisymmetric, in this case on the  $y = 0$  plane. Such a conducting sheet forces the electric field to have only a  $y$  component there. Of course, such a sheet cannot extend to infinity but must be truncated at dimensions comparable to the rest of the antenna so that this sheet does not become the dominant factor in the antenna size (the antenna aperture being the most important factor in antenna size). In this context, then the width of this sheet can appropriately have the full width of the reflector on the  $y = 0$  plane and electrically bonding to the reflector continuously across this width. In the  $+z$  direction the sheet can extend to include the focal region.

The presence of such a conducting sheet gives some additional flexibility in the design of the cable connections near the focus. Consider the connection to arm pair 3 and 4 (negative  $y$  in Figs. 2.1 and 2.2) as illustrated in Fig. 3.1. The presence of the ground plane allows one to reroute the  $100 \Omega$  cable from the  $z$  axis to a more general path on the  $y = 0$  plane. In particular, the cable can be routed around to the opposite side ( $+z$  side) of the paraboloidal focus so as to launch the wave from the coax in the direction toward the reflector. The coax shield can be opened in a gradual manner so as to smoothly transition from a coax to an asymmetrical strip line (also called an zipper [15]) while maintaining the same characteristic impedance ( $100 \Omega$  in this case) at every cross section. The coax shield blending into the ground plane, the wave from the coax is next launched on the conical transmission line consisting of arms 3 and 4 and the ground plane. The region near the focus is now clear of scatterers (such as cable shields) in the direction toward the reflector. Note that the  $100 \Omega$  coax should be bonded (frequently electrically connected) to the ground plane, and perhaps even recessed into the ground plane to better preserve the  $R_y$  symmetry of the overall antenna. (One could also include a dummy cable at the opposite  $x$  coordinate (positive  $x$  in Fig. 3.1) to better maintain  $R_x$  symmetry.)

This still leaves various details of the focal region to optimize. The two arms 3 and 4 need to connect to the coax center conductor with as little distortion of the spherical TEM wave in the focal region as possible. Launching from the strip line with its dielectric insulation onto an air-dielectric conical transmission line brings into consideration the dielectric/air boundary, a lens-design consideration.

Comparing the focal-region design for negative  $y$  to that for positive  $y$  (the other side of the ground plane) there are significant differences. The  $100 \Omega$  cable has been shifted away from the  $z$  axis, clearing up the focal region here as well. (See Fig. 2.2.) The  $100 \Omega$  cable on arm 2 now has its center conductor connected to the ground plane on the  $+y$  side. This then leaves the question of the details of how the coax center conductor leaves the coax and transitions to the ground plane in a way which minimizes the distortion of the spherical TEM wave to be launched. Note now that the wave from the coax has to change direction (bend) back toward the reflector, a bend of typically greater than  $\pi/2$  ( $90^\circ$ ) [8]. On the inside of the bend (toward the reflector) the wave should propagate slower than on the outside, another lensing problem.

#### 4. Symmetry Between Electric and Magnetic Dipoles for Low-Frequency Performance

Another kind of symmetry is duality, an invariance to interchange for electric and magnetic parameters in the Maxwell equations [17]. A special case of this concerns the electric and magnetic dipoles describing the low-frequency antenna performance. As shown in [1] there is a special balance between the dipoles in which each contributes equally to the fields and gives special properties to the fields. In the coordinates of Fig. 2.1 we have the balance conditions

$$\begin{aligned}
 \vec{p} &= p \hat{1}_y && \text{(electric moment)} \\
 \vec{m} &= -m \hat{1}_x && \text{(magnetic moment)} \\
 p &= \frac{m}{c} && (4.1) \\
 \hat{1}_c &= \hat{1}_z && \text{(direction of beam center in transmission)} \\
 c &= [\mu_o \epsilon_o]^{-\frac{1}{2}} && \text{(speed of light)}
 \end{aligned}$$

This assures a cardioid pattern centered on the +z axis [6] and makes electric and magnetic fields on the z axis have the ratio  $Z_o$  (wave impedance of free space  $\approx 377\Omega$ ), even including the near-field dipole terms.

As discussed in [4] the resistive terminations at the reflector approximately give the balance conditions, making the low-frequency radiation maximized in the +z direction. For long focal lengths compared to reflector diameter (large  $F/D$ ) a transmission-line model of the terminated feed gives exactly the  $p = m/c$  condition [2, 3]. (The symmetry gives the vector orientations exactly.) However, for realistic values of  $F/D$  [8], the match is not perfect. The charge on the feed arms produces an electric-dipole moment which is partly cancelled (shielded) by the charge distribution induced on the reflector. Calculations of this are contained in [7]. Detailed calculations including reflector and feed-arm detailed shapes are also needed.

One can consider modifications to the design for improving the low-frequency electric/magnetic balance, such as illustrated in Fig. 4.1. Here one modifies each feed arm in the region beyond a distance  $F$  from the focus [8]. Besides the terminating resistor  $R_t$  (typically  $200\Omega$ ) one may add a special feedlet (armlet or whatever, analogous to winglet), the purpose of which is to extend the charge on the feed arm to distances farther from the z axis and thereby increase the low-frequency electric-dipole moment. This feedlet might be resistive (sheet resistance  $R_s$ ) so as to let the low-frequency magnetic field penetrate and thereby not change the low-frequency magnetic-dipole moment. This can also absorb some of the electromagnetic energy that would otherwise contribute to a sidelobe in the direction of the feed arm. This feedlet can have various geometries, even extending behind the reflector. It may even be comprised of anisotropic (e.g., uniconducting) materials.

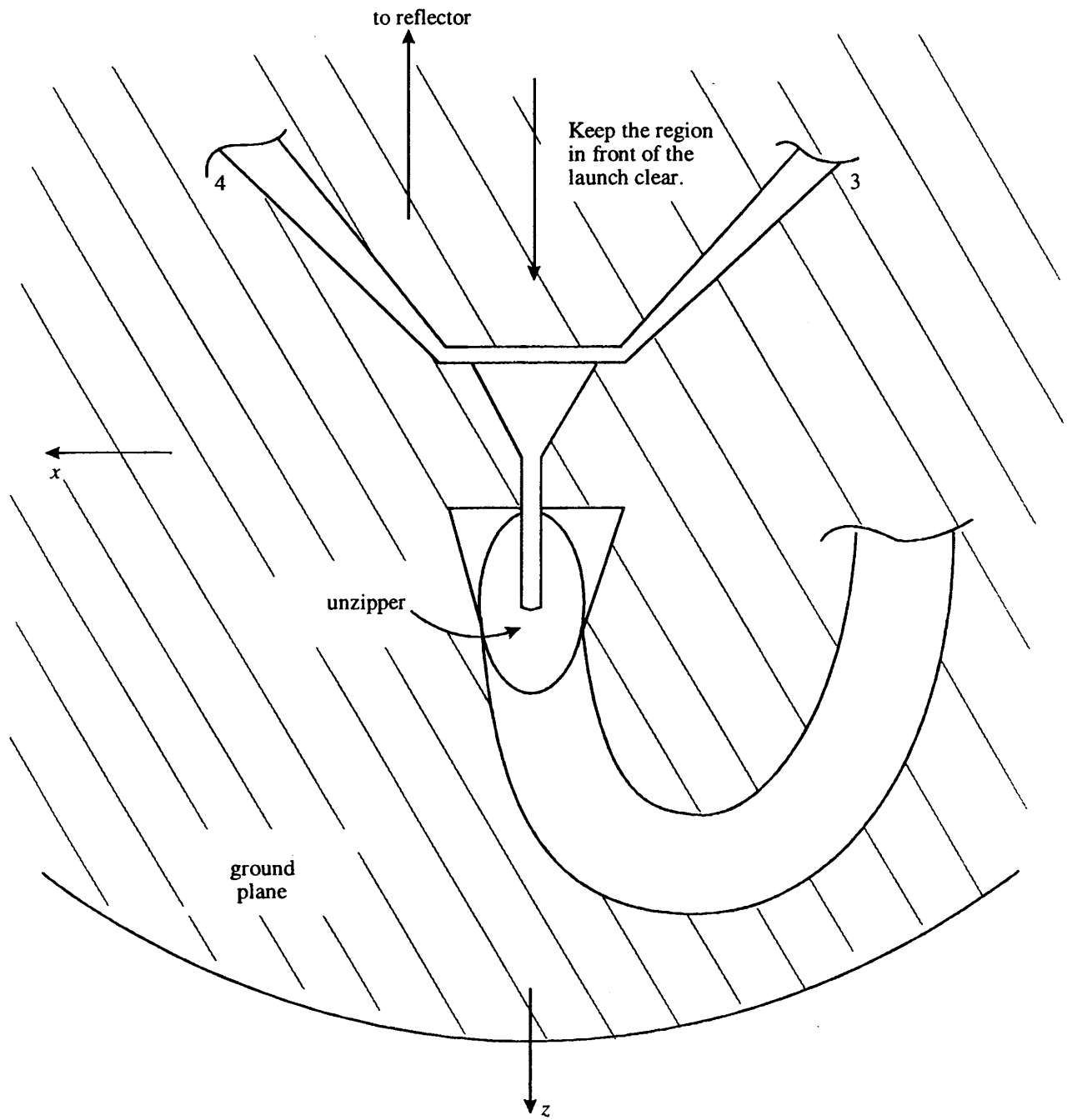
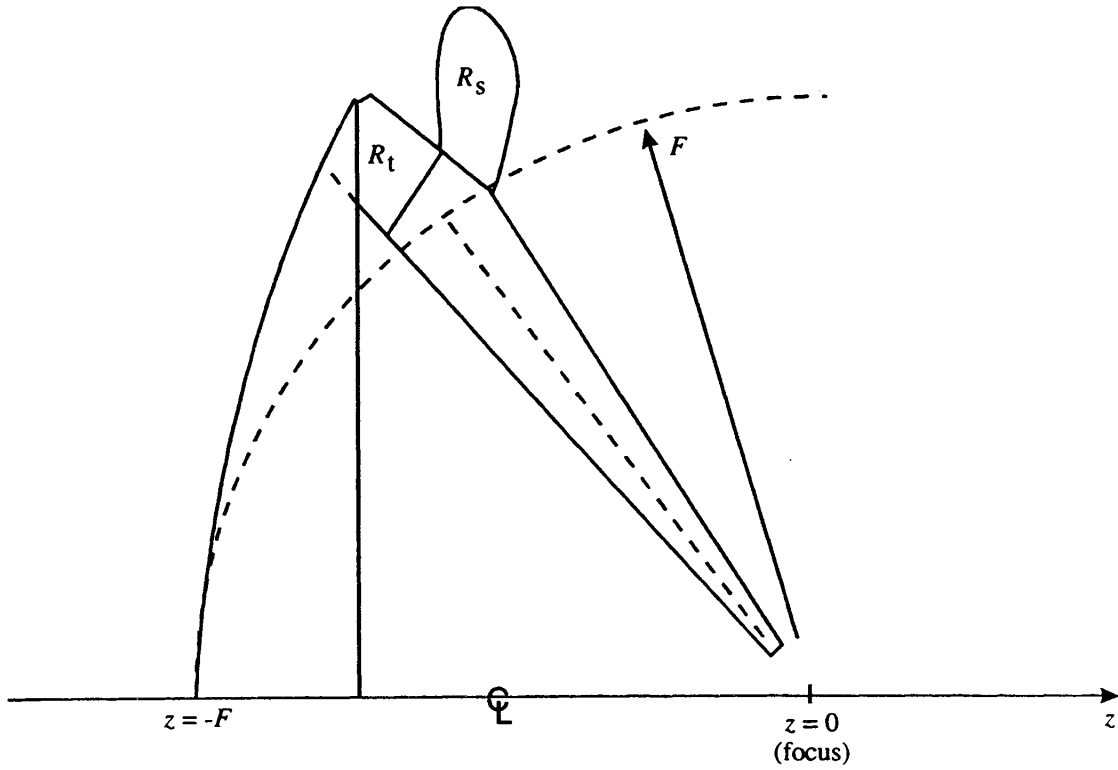


Fig. 3.1 Focal Region With Ground Plane For Arm Pair 3 and 4



Only one feed arm (typical) is shown

Fig. 4.1 Feedlets for Balancing Electric- and Magnetic-Dipole Moments.

Note that the introduction of non-circular reflector truncation to give other antenna apertures (e.g., rectangular) further complicates the low-frequency electric/magnetic balancing problem. Detailed calculations of both moments, including the effects of various feedlet designs would help considerably. Experiments with tuning for the low-frequency null in the  $-z$  direction may also help.

## 5. Concluding Remarks

There are lots of little things to include in a reflector-IRA design to make its ideal performance more closely approximated. This paper has discussed several such improvements. Detailed calculations and experimental optimization are appropriate. For the small structures in the focal region, these can be investigated experimentally by inverse scale models (structures many times larger than the actual desired sizes).

In this paper we have referred to  $50 \Omega$  and  $100 \Omega$  coaxes. While these are convenient choices they can, in principle, take on other values. For present purposes, these numbers are labels.

## References

1. C. E. Baum, Some Characteristics of Electric and Magnetic Antennas for Radiating Transient Pulses, Sensor and Simulation Note 125, January 1971.
2. J. S. Yu, C.-L. Chen, and C. E. Baum, Multipole Radiations: Formulation and Evaluation for Small EMP Simulators, Sensor and Simulation Note 243, July 1978.
3. E. G. Farr and J. S. Hofstra, An Incident Field sensor for EMP Measurements, Sensor and Simulation Note 319, November 1989; IEEE Trans. EMC, 1991, pp. 105-112.
4. C. E. Baum, Radiation of Impulse-Like Transient Fields, Sensor and Simulation Note 321, November 1989.
5. C. E. Baum, Configurations of TEM Feed for an IRA, Sensor and Simulation Note 327, April 1991.
6. C. E. Baum, General Properties of Antennas, Sensor and Simulation Note 330, July 1991.
7. D. V. Giri and S. Y. Chu, On the Low-Frequency Electric Dipole Moment of Impulse Radiating Antennas (IRAs), Sensor and Simulation Note 346, October 1992.
8. C. E. Baum, Some Topics Concerning Feed Arms of Reflector IRAs, Sensor and Simulation Note 414, October 1997.
9. C. E. Baum, Selection of Angles Between Planes of TEM Feed Arms of an IRA, Sensor and Simulation Note 425, August 1998.
10. C. E. Baum, Symmetry and SAR Antennas, Sensor and Simulation Note 431, November 1998.
11. C. E. Baum, Unipolarized Currents for Antenna Polarization Control, Sensor and Simulation Note 437, June 1999.
12. J. Scott Tyo, Optimization of the Feed Impedance for an Arbitrary Crossed-Feed-Arm Impulse Radiating Antenna, Sensor and Simulation Note 438, November 1999.
13. C. E. Baum, Optimization of Reflector IRA Aperture for Filling a Rectangle, Sensor and Simulation Note 439, September 1999.
14. C. E. Baum, Interaction of Electromagnetic Fields With an Object Which Has an Electromagnetic Symmetry Plane, Interaction Note 63, March 1971.
15. G. D. Sower, L. M. Atchley, and D. E. Ellibee, Low-Voltage Prototype Development of an Ultra-Wideband High-Voltage Unzipper Balun, Measurement Note 50, December 1996.
16. C. E. Baum, Electromagnetic Sensors and Measurement Techniques, pp. 73-144, in J. E. Thompson and L. H. Luessen (eds.), *Fast Electrical and Optical Measurements*, Martinus Nijhoff, Dordrecht, 1986.
17. C. E. Baum and H. N. Kritikos, Symmetry in Electromagnetics, Ch. 1, pp. 1-90, in C. E. Baum and H. N. Kritikos (eds.), *Electromagnetic Symmetry*, Taylor & Francis, 1995.
18. C. E. Baum, E. G. Farr, and D. V. Giri, Review of Impulse-Radiating Antennas, Ch. 16, pp. 403-439, in W. R. Stone (ed.), *Review of Radio Science 1996-1999*, Oxford U. Press, 1999.